CAPACITANCE CALCULATION USING EEM

Slavoljub R. ALEKSIĆ, Mirjana PERIĆ, Saša S. ILIĆ
Department of Theoretical Electrical Engineering, Faculty of Electronic Engineering,
University of Niš, Aleksandra Medvedeva 14, 18000 Niš, Serbia, tel. +381 18 529 423, E-mail: mika@elfak.rs

ABSTRACT

Sometimes physical systems can be so complex that analytical solutions for potentials or electric fields strength of those problems are difficult or even impossible to be found. Fortunately, with the application of the computer, it is now possible to use simple numerical approximation methods to solve more complex problems in a matter of a few minutes. For determination an unknown capacitance can be used different numerical methods. In this article, the Equivalent Electrodes Method (EEM) [9] is used for calculation of system capacitance. A sphere and thin ring form this system. In paper [5], the authors called that system "Saturn" capacitor. In this article, the capacitance of this system, when the capacitor ring has finite or negligible thickness is calculated. Also, the ring cross-section can have different shapes. The capacitance calculation has been done for several ring cross-section shapes. The Equivalent Electrodes Method, Point-matching Method and Image theorem are used for calculation. The convergence of the results will be shown in the tables, and the capacitance values for different values of parameters will be shown graphically. Also, the obtained results for capacitance for different ring cross-section shapes will be shown in the tables.

In last few years there has been developed a large number of software packages for solving problems in Electromagnetics. They make calculations easier and it is also a good way to confirm the results obtained by some analytical or numerical method. In this article, the obtained EEM results will be compared with FEMM software [10] results.

Keywords: *Capacitance calculation, Equivalent Electrodes Method (EEM), Point-matching Method (PMM), Image theorem, Finite Element Method (FEM).*

1. INTRODUCTION

A sphere of radius a and a thin ring with negligible or finite thickness, having inner radius b and exterior radius c, form so-called "Saturn" capacitor [5]. The ring is at the potential U, the sphere is at the potential V and placed at the height h, Fig. 1.

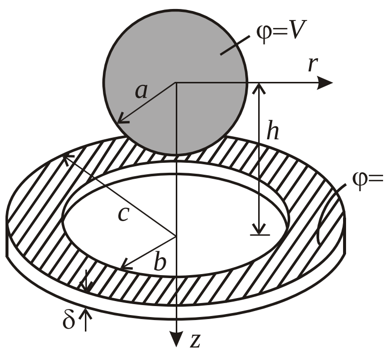

Fig. 1 "Saturn" capacitor.

The most common method for electrophysiological investigation for ion channel proteins is the two-microelectrode voltage clamp technique [3], Fig. 2. A spherical electrode and a thin ring electrode form one part of that system i.e. "Saturn" capacitor.

In references [2, 5, 6] a capacitance of the "Saturn" capacitor is considered. In papers [2, 5] a thin ring with a negligible thickness has been observed. In the paper [6] the ring has had a finite thickness. In that case, the ring shape cross-section was rectangular. An influence of different ring cross-section shapes is considered in the paper [7].

In this paper will be presented all obtained results and those results will be compared with the Finite Element Method (FEM) results.

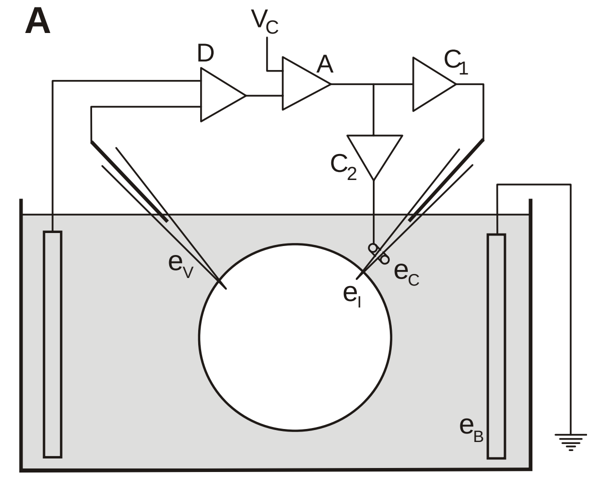

Fig. 2 Two-microelectrode voltage clamp system.

2. EQUIVALENT ELECTRODES METHOD (EEM)

This method has been developed at the Faculty of Electronic Engineering in Niš - Department of Theoretical Electrical Engineering and it belongs to the group of Semi Numerical Methods. The first very good results were obtained in [8], when this method is used for calculating the equivalent radius of uniform antennas. A basic idea of this method is replacing an electrostatic system by a finite system of equivalent electrodes (EEs) [9].

The equivalent electrodes of different shapes can be used depending on the problem geometry. The flat or oval strips (for plan-parallel problems), spherical bodies (for three-dimensional problems) or toroidal electrodes (for systems with axial symmetry) can be commonly used.

The equivalent electrodes potential should be equal to the real electrode potential. The system of linear equations is formed using this boundary condition, with equivalent electrodes charges as unknown values. After solving this system, the unknown charges of EEs can be determined. Using standard formulas the potential, the electric field strength and the capacitance of the system can be computed.

The EEM has a wide range of applications [9]. This method was applied in computation of electrostatic fields, in theory of low-frequency grounding systems, in the magneto static field and heat flow problems solving, transmission line analysis, etc.

In [10], this method is applied for electric field and potential determination at the coaxial cable terminations and joints. Toroidal electrodes are used as EEs. In [11] the EEs are small spherical bodies used to determine the atmospheric electric field distribution in the surroundings of the vehicles. A potential distribution in vicinity of biological bodies exposed to ELF electric field is determined in [12] using the EEs of identical shape as in [11]. Flat or oval strips elements of large length and neglected width can be used as the EEs for electromagnetic field analysis which slit coaxial lines produce in tunnels and in bridges with one or double track [13].

3. EEM APPLICATION

3.1. Ring with negligible thickness

For determination the capacitance of the system from Fig. 1, when the ring has a negligible thickness ($\delta \to 0$), the ring is divided in N strips, Fig. 3 [1].

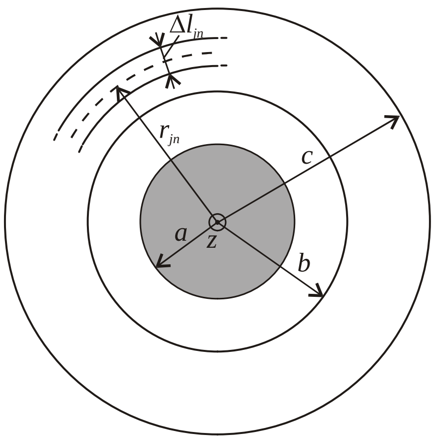

Fig. 3 EEM application.

The radius of n-th strip is

$$r_n = 0.5b\left[\left(\frac{c}{b}\right)^{n/N} + \left(\frac{c}{b}\right)^{(n-1)/N}\right], \tag{1}$$

and its width is

$$\Delta l_n = b\left[\left(\frac{c}{b}\right)^{n/N} - \left(\frac{c}{b}\right)^{(n-1)/N}\right]. \tag{2}$$

Each of the formed strips can be replaced by equivalent loops, having radius r_n, with the circular cross-section of radius $a_{en} = \Delta l_n / 4$.

The sphere and N loops form the system. Applying the image theorem in the sphere mirror, the equivalent system is formed. The charges of the loops, their images in the sphere mirror and one point charge placed in the centre of the sphere form this system, Fig. 4.

The images are loops, too, with radii

$$r'_n = r_n\left(\frac{a}{d_n}\right)^2, \tag{3}$$

and

$$Q'_n = -\frac{a}{d_n}Q_n \tag{4}$$

is charge of the n-th loop image.

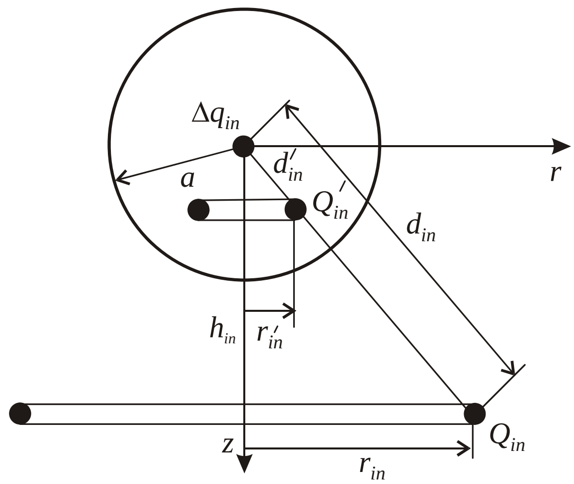

Fig. 4 Equivalent system.

The ring and the sphere form a capacitor, so their charges must be equal, but of the opposite sign. Because of that, the total sphere charge must be $-Q$ [14]. One part of this charge is divided into image charges, obtained using image theorem. The influence of these charges can be presented with one equivalent loop, and the other charges

$$\Delta q_n = -Q_n - Q'_n = -\left(1 - \frac{a}{d_n}\right)Q_n \tag{5}$$

are uniformly placed at the sphere surface, so their influence can be presented with point charge placed in the centre of the sphere. Its intensity is

$$\Delta q = \sum_{n=1}^{N} \Delta q_n \,. \tag{6}$$

The potential in point $\mathrm{M}(r,z)$ is

$$\varphi=\sum_{n=1}^{N}\frac{1}{2\pi^2\varepsilon}\left[Q_n\frac{\mathrm{K}\left(\frac{\pi}{2},k_n\right)}{\sqrt{(r+r_n)^2+(z-h)^2}}+\right.$$

$$+Q_n'\frac{\mathrm{K}\left(\frac{\pi}{2},k_n'\right)}{\sqrt{(r+r_n')^2+\left(z-h\left(\frac{a}{d_n}\right)^2\right)^2}}+$$

$$\left.+\frac{\pi}{2}\frac{\Delta q_n}{\sqrt{r^2+z^2}}\right], \qquad (7)$$

where $\mathrm{K}\left(\frac{\pi}{2},k_n\right)$ and $\mathrm{K}\left(\frac{\pi}{2},k_n'\right)$ are complete elliptic integrals of the first kind, with modules

$$k_n^2=\frac{4rr_n}{(r+r_n)^2+(z-h)^2}$$

and

$$k_n'^2=\frac{4rr_n'}{(r+r_n')^2+\left(z-h\left(\frac{a}{d_n}\right)^2\right)^2}.$$

When the potential in some point $\mathrm{M}(r,z)$ is matched in N matching points placed at the electrodes surfaces, the system of linear equations is formed:

$$U=\sum_{n=1}^{N}\frac{Q_n}{2\pi^2\varepsilon}\left[\frac{\mathrm{K}\left(\frac{\pi}{2},k_{mn}\right)}{\sqrt{(r_m+r_n)^2+\delta_{mn}a_{em}^2}}-\right.$$

$$-\frac{a}{d_n}\frac{\mathrm{K}\left(\frac{\pi}{2},k_{mn}'\right)}{(r_m+r_n')^2+h^2\left(1-\left(\frac{a}{d_n}\right)^2\right)^2}-$$

$$\left.-\frac{\pi}{2\sqrt{r_m^2+h^2}}\left(1-\frac{a}{d_n}\right)\right],\quad m=1,2,\ldots,N, \qquad (8)$$

where δ_{mn} is Kronecker symbol.

$$k_{mn}^2=\frac{4r_mr_n}{(r_m+r_n)^2+\delta_{mn}a_{em}^2}\ \text{and}$$

$$k_{mn}'^2=\frac{4r_mr_n'}{\left(r_m+r_n'\right)^2+h^2\left(1-\left(\frac{a}{d_n}\right)^2\right)^2}$$

are modules of the elliptic integrals.

After solving system (8) the capacitance can be calculated as

$$C=\frac{Q}{U-V} \qquad (9)$$

where

$$Q=\sum_{n=1}^{N}Q_n \qquad (10)$$

is the total charge of the ring electrode.

The sphere potential, denoted with V, derives from the charge Δq, placed in the centre of the sphere. Using condition that the sphere is equipotential this potential can be determined:

$$\frac{V}{U}=-\frac{\pi}{2}\sum_{n=1}^{N}\left(1-\frac{a}{r_n}\right)\frac{Q_n}{2\pi^2\varepsilon a}. \qquad (11)$$

3.2. Ring with finite thickness

A problem is more complex when the ring has finite thickness. In that case, all four sides of the ring cross-section should be divided in strips.

Upper and bottom sides of the ring cross-section are divided in the same way as in the case of the ring with the negligible thickness. But, number of the equivalent electrodes on the upper and bottom ringsides can be different. So, the ring is divided in N_j strips using expressions (1) and (2) [14], where $j=1,2$.

Indexes 1 and 2 correspond to the strips on the upper and bottom ringside, respectively.

Depends on the ring cross-section shape, inner and exterior sides can be divided in different ways. If the ring cross-section shape is rectangular, Fig. 5, inner and exterior sides, with radii $r=b$ and $r=c$, have been divided in $N_3=N_4$ ring strips, with width

$$\Delta l_{kn}=\frac{\delta}{N_k}, \qquad (12)$$

($n=1,\ldots,N_3$), placed at positions

$$h_{kn}=h-\frac{\delta}{2}+(2n-1)\frac{\Delta l_{kn}}{2}. \qquad (13)$$

where $k = 3,4$. Indexes 3 and 4 correspond to inner ($r_{3n} = b$) and exterior ($r_{4n} = c$) ringside, respectively. Each of the formed strips can be replaced by equivalent loops, having radius r_{kn} with circular cross-section of radius $a_{\mathrm{e}kn} = \Delta l_{kn}/4$, $k = 1,2,3,4$.

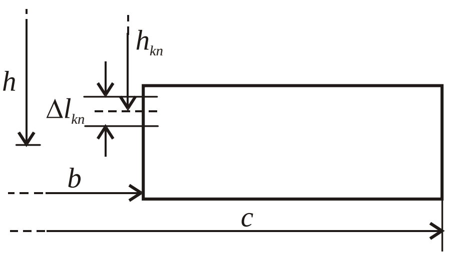

Fig. 5 Rectangular shape of the ring cross-section.

If the inner and exterior sides of ring cross-section are half circular, with radius $\delta/2$, Fig. 6, they will be divided in $N_3 = N_4$ strips with width $\delta\Delta\theta/2$, where

$$\Delta\theta = \frac{\pi}{N_k} \tag{14}$$

where $k = 3,4$. Indexes 3 and 4 correspond to inner and exterior sides of ring cross-section, respectively.

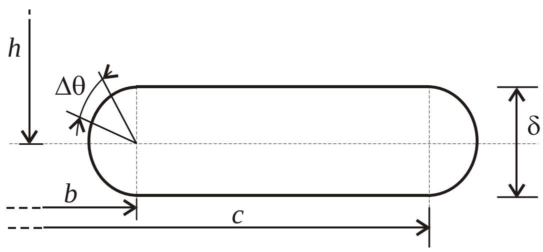

Fig. 6 Shape of the ring cross-section.

Each of the formed strips can be replaced by equivalent loops with circular cross-section of radius

$$a_{\mathrm{e}kn} = \frac{\delta}{2}\sin\left(\frac{\Delta\theta}{4}\right).$$

The radii of formed strips are

$$r_{kn} = b - \frac{\delta}{2}\cos\theta_{kn} \text{ and} \tag{15}$$

$$r_{kn} = c + \frac{\delta}{2}\cos\theta_{kn}, \tag{16}$$

for inner and exterior sides of ring cross-section, respectively. The normal distance of these strips from the sphere centre is

$$h_{kn} = h - \frac{\delta}{2}\sin\theta_{kn}, \tag{17}$$

where

$$\theta_{kn} = \frac{\pi}{2N_k}(2n - 1 - N_k), \tag{18}$$

($n = 1,2,\ldots,N_k$ and $k = 3,4$).

Application of previous expressions depends on the ring cross-section shape. If the exterior side of ring cross-section is flat, the strips will be formed using the expression (12). If the inner side is half circular, the strips will have the positions described using the expressions (15) and (17).

For any ring cross-section shape, the sphere and N loops, where $N = N_1 + N_2 + N_3 + N_4$, form the system.

Applying the image theorem in the sphere mirror, the equivalent system is formed as in chapter 3.1. The charges of the loops, their images in the sphere mirror and one point charge placed in the centre of the sphere form this system. In this case only the number of equivalent electrodes is different. Also, the number of images is bigger.

The potential at point $\mathrm{M}(r,z)$ is

$$\varphi = \sum_{i=1}^{4}\sum_{n=1}^{N_i}\frac{1}{2\pi^2\varepsilon}\left[Q_{in}\frac{\mathrm{K}\left(\frac{\pi}{2},k_{in}\right)}{\sqrt{(r+r_{in})^2+z^2}} + Q'_{in}\frac{\mathrm{K}\left(\frac{\pi}{2},k'_{in}\right)}{\sqrt{(r+r'_{in})^2+z^2}} + \frac{\pi}{2}\frac{\Delta q_{in}}{\sqrt{r^2+z^2}}\right], \tag{19}$$

where $\mathrm{K}\left(\frac{\pi}{2},k_{in}\right)$ and $\mathrm{K}\left(\frac{\pi}{2},k'_{in}\right)$ are complete elliptic integrals of the first kind, with modulus

$$k_{in}^2 = \frac{4rr_{in}}{(r+r_{in})^2+z^2} \text{ and } k_{in}'^2 = \frac{4rr'_{in}}{(r+r'_{in})^2+z^2},$$

and $Q'_{in} = -\frac{a}{r_{in}}Q_{in}$ is charge of the n-th loop image ($i = 1,2,3,4$).

With Δq_{in} ($i = 1,2,3,4$) the point charges placed in the centre of the sphere are denoted. Parameter N_i ($i = 1,2,3,4$) corresponds to the equivalent electrodes number of each ringside.

The unknown charges Q_{in} can be determined when the potential (19) is matched in N matching points placed at the electrodes surfaces.

After solving formed system of linear equations the capacitance can be calculated.

4. NUMERICAL RESULTS

In Table 1 and Table 2, the capacitance values, for different number of equivalent electrodes (EEs) and different values of the parameters, are shown. Those results are presented for the ring with the negligible thickness.

Table 1 Normalized capacitance for different number of EEs, for $b/a = 1.5$, $h/a = 1.0$ and

	$c/a = 2.5$	$c/a = 8.0$
N	$C/2\pi^2\varepsilon a$	$C/2\pi^2\varepsilon a$
20	0.822387810001	0.755306923094
30	0.821834725333	0.754993298392
50	0.821313034730	0.754783322516
100	0.820842802590	0.754667353520
150	0.820659718595	0.754642755134
200	0.820560021664	0.754663485378

The obtained results have shown that small number of the equivalent electrodes, the good convergence of the results.

Table 2 Normalized capacitance for different number of EEs, for $b/a = 1.5$, $h/a = 8.0$ and

	$c/a = 2.5$	$c/a = 8.0$
N	$C/2\pi^2\varepsilon a$	$C/2\pi^2\varepsilon a$
20	0.452348182622	0.637047922345
30	0.452225635291	0.636923436253
50	0.452086095869	0.636789099615
100	0.451940052984	0.636650600848
150	0.451877563907	0.636591167078
200	0.451842043759	0.636557226094

In Figs. 7 and 8, the capacitance values for different parameters are shown. The number of the EEs is $N = 100$. These results are presented for the negligible ring thickness.

From Fig. 7, it is evident that when distance between the ring and the sphere increases and the ring width decreases, the capacitance values stream to identical value. That is because the sphere doesn't "see" the ring width. When the distance between the sphere and the ring increases, the capacitance is almost constant. That can be seen from Fig. 8.

In Table 3 and Table 4, the capacitance values, for different number of the equivalent electrodes and different values of parameters, are shown. The ring has a finite thickness and the ring cross-section shape is rectangular as in Fig. 5. From these tables the good convergence of the results can be noticed.

The ring thickness is given using the parameter Δ, where

$$\Delta = \frac{\delta}{c-b}. \tag{20}$$

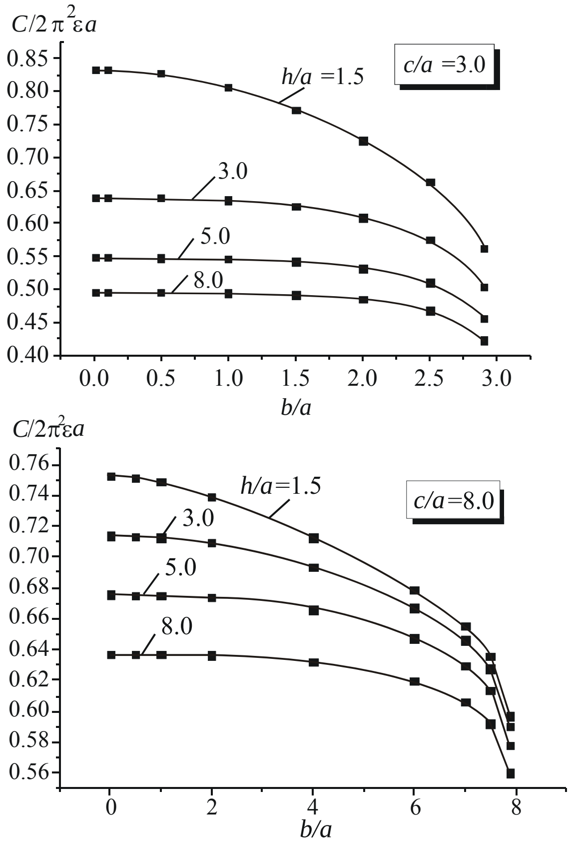

Fig. 7 Capacitance versus parameter b/a.

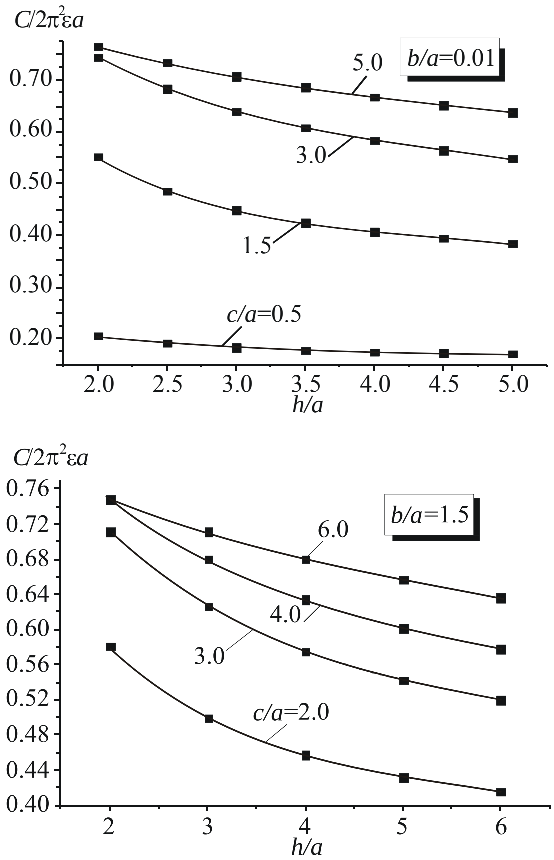

Fig. 8 Capacitance versus parameter h/a.

Table 3 Capacitance for different number of EEs, for $b/a = 2.0$, $c/a = 3.0$ and $h/a = 0.0$.

$\Delta = 0.01$		$\Delta = 0.1$	
N	$C/2\pi^2\varepsilon a$	N	$C/2\pi^2\varepsilon a$
20	0.8517249114	20	0.8906905258
30	0.8591924056	30	0.8895970007
50	0.8615284292	50	0.8886667993
80	0.8617913541	80	0.8882241875
100	0.8617266748	100	0.8880980130
150	0.8615377676	150	0.8878836563
200	0.8614092168	200	0.8877595248

In Tables 5-8, the capacitance values for different shapes of ring cross-section and different values of parameters are shown. The rectangular cross-section is "Shape 1". For "Shape 2" the inner side is half circular and exterior side of ring cross-section is flat. "Shape 3" corresponds to the shape presented in Fig.6.

Table 4 Capacitance for different number of EEs, for $b/a = 2.0$, $c/a = 3.0$ and $h/a = 1.0$.

$\Delta = 0.01$		$\Delta = 0.1$	
N	$C/2\pi^2\varepsilon a$	N	$C/2\pi^2\varepsilon a$
20	0.7847170894	20	0.8165307862
30	0.7908987714	30	0.8154089370
50	0.7926265740	50	0.8145657420
80	0.7931838896	80	0.8141692807
100	0.7931068251	100	0.8140549214
150	0.7929422077	150	0.8138765474
200	0.7928340829	200	0.8137751744

Table 5 Capacitance for different ring cross-section shapes, for $b/a = 2.0$, $c/a = 3.0$ and $h/a = 0.0$.

$N = 200$	$C/2\pi^2\varepsilon a$		
Δ	Shape 1	Shape 2	Shape 3
0.01	0.86140922	0.86251650	0.86284000
0.05	0.87442003	0.88019209	0.88164570
0.10	0.88775952	0.89935978	0.90184113
0.15	0.89951629	0.91740597	0.92068939
0.20	0.91024679	0.93494090	0.93885055

From these tables it can be found that if the distance between the sphere and the ring increases, the difference between capacitance results for different shapes of ring cross-section decreases.

Also, the bigger ring thickness, the bigger capacitance value is obtained. The smallest capacitance values are for the "Shape 1". When both sides of the ring cross-section are of half circular shape ("Shape 3"), the capacitance values are the biggest.

Table 6 Capacitance for different ring cross-section shapes, for $b/a = 2.0$, $c/a = 3.0$ and $h/a = 0.5$.

$N = 200$	$C/2\pi^2\varepsilon a$		
Δ	Shape 1	Shape 2	Shape 3
0.01	0.84128101	0.84225911	0.84258872
0.05	0.85343273	0.85849666	0.85998528
0.10	0.86592667	0.87603187	0.87858828
0.15	0.87696743	0.89245478	0.89585774
0.20	0.88707376	0.90833128	0.91240785

Table 7 Capacitance for different ring cross-section shapes, for $b/a = 2.0$, $c/a = 3.0$ and $h/a = 1.0$.

$N = 200$	$C/2\pi^2\varepsilon a$		
Δ	Shape 1	Shape 2	Shape 3
0.01	0.79283408	0.79354619	0.79389070
0.05	0.80313199	0.80675523	0.80833047
0.10	0.81377517	0.82087548	0.82361947
0.15	0.82322328	0.83393232	0.83763635
0.20	0.83191439	0.84639990	0.85089954

Table 8 Capacitance for different ring cross-section shapes, for $b/a = 2.0$, $c/a = 3.0$ and $h/a = 5.0$.

$N = 200$	$C/2\pi^2\varepsilon a$		
Δ	Shape 1	Shape 2	Shape 3
0.01	0.53392498	0.53402733	0.53436686
0.05	0.53830085	0.53876972	0.54040538
0.10	0.54276475	0.54358484	0.54660431
0.15	0.54667231	0.54778650	0.55209139
0.20	0.55022101	0.55158615	0.55709905

From Table 8 it is evident that an influence of the ring thickness is negligible. When the distance between the ring and the sphere is large, the sphere doesn't "see" the ring thickness. The distance between the EEs placed on the ringsides and their images in the sphere is approximately equal. That is the reason why the ring thickness hasn't influence on the system capacitance.

In Figs. 9-10 the capacitance values for different parameters values are shown. All presented results are obtained when ring cross-section has the "Shape 1". In Fig. 9 the capacitance dependence versus ring thickness, i.e. parameter Δ, when b/a and c/a have constant values, is shown. From Fig. 9b it is evident that when the distance between the ring and the sphere increases and the ring has bigger thickness, the capacitance has constant value. As it is mentioned, in that case, the sphere doesn't "see" the ring thickness, so the capacitance is constant.

The capacitance values for thin ring with the negligible thickness and the ring with the finite thickness have been compared in Fig. 10.

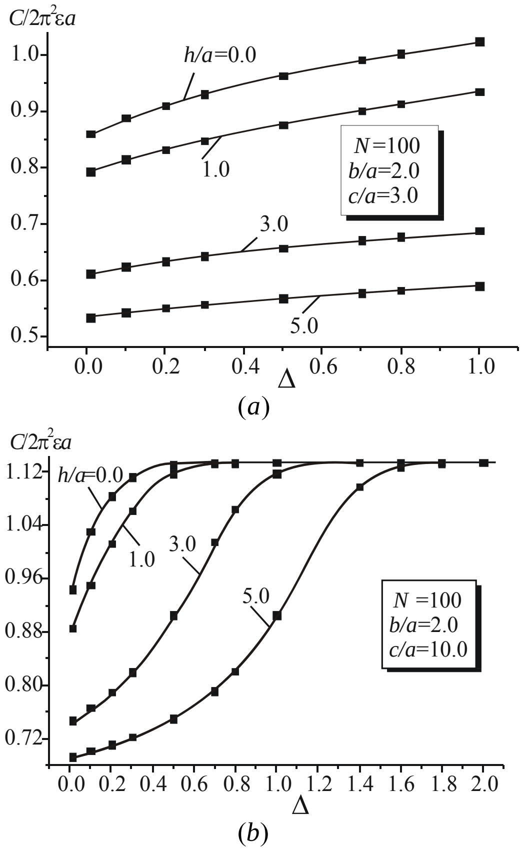

Fig. 9 Capacitance dependence versus parameter Δ for different values of parameter h/a.

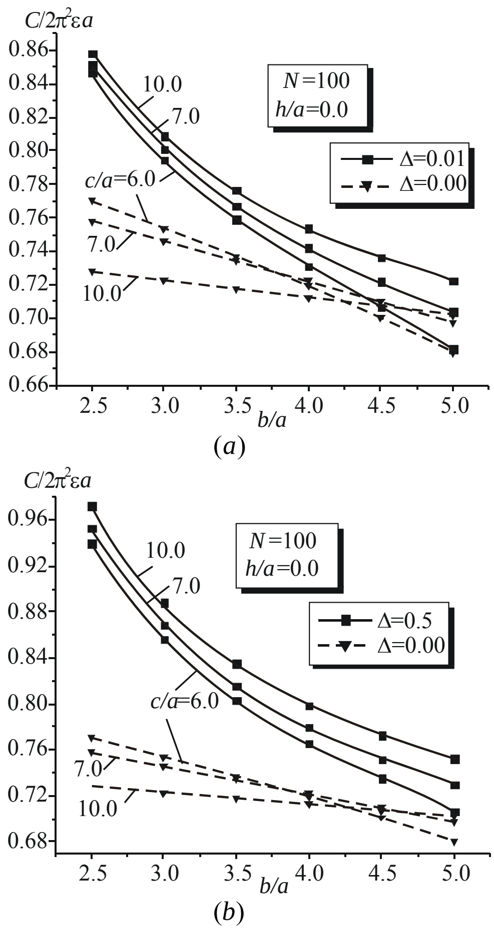

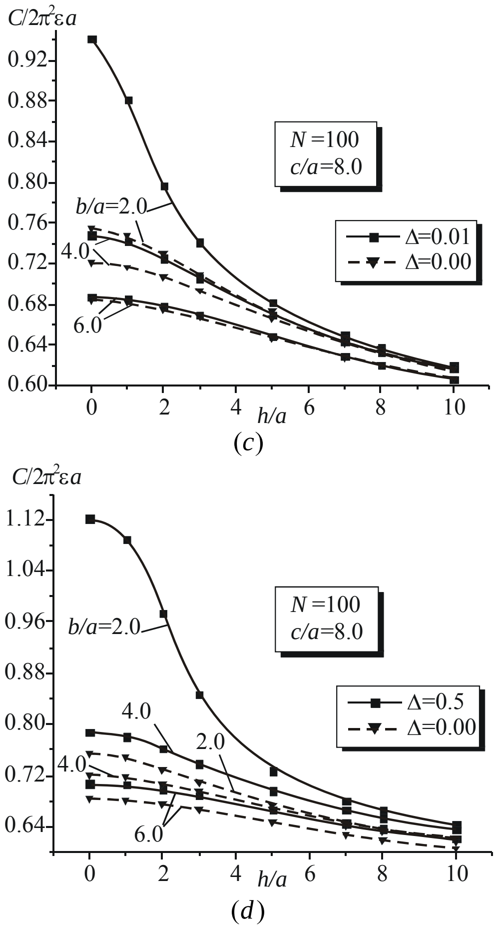

Fig. 10 Results comparison for different ring thickness and different values of parameters.

From Figs. 10c and 10d, it can be seen that when the distance between ring and sphere increases, the capacitance values stream to equal value.

In Fig. 11, the equipotential curves, obtained using software package [4], are shown.

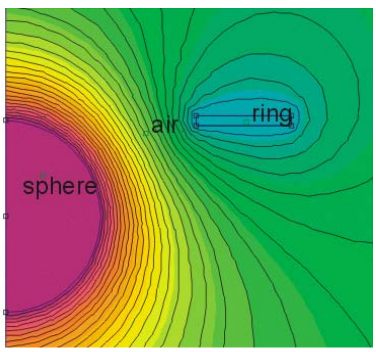

Fig. 11 Equipotential curves (FEMM 4.0) for $b/a = 2.0$, $c/a = 3.0$ and $h/a = 1.0$.

In Tables 9-10, the EEM results have been compared with FEM results. FEM values are obtained using FEMM software package [4]. The ring cross-section shape is rectangular. The number of EEs in EEM is $N = 200$. From these tables the good results agreement can be noticed (an error rate is less than 0.5 %).

Table 9 Capacitance values comparison, for $b/a = 2.0$, $c/a = 3.0$ and $h/a = 0.0$.

	$C/2\pi^2\varepsilon a$	
Δ	EEM	FEM
0.00	0.82815312	0.86051667
0.01	0.86140922	0.86031416
0.10	0.88775952	0.88794107
0.20	0.91024679	0.90973715

Table 10 Capacitance values comparison, for $b/a = 2.0$, $c/a = 3.0$ and $h/a = 2.0$.

	$C/2\pi^2\varepsilon a$	
Δ	EEM	FEM
0.00	0.68018716	0.68509607
0.01	0.68668157	0.68521170
0.10	0.70134705	0.70027710
0.20	0.71407189	0.71278599

5. CONCLUSION

The obtained results have shown that when the number of equivalent electrodes is small ($N = 50$), the good convergence of the results is achieved. When the distance between the ring and the sphere increases, for any ring cross-section shape, the capacitance has approximately a constant value.

The EEM results are obtained using a program written in FORTRAN 77. The CPU calculation time is connected with the total number of the EEs. When the number of EEs increases, the CPU time increases too. But this calculation time is not so significant. All necessary calculations have been done only for a few seconds. All calculations are carried out on a PC with 256 MB RAM, 1.6GHz.

The EEM results have been compared with the FEM results. The excellent results agreements have been obtained. The ring is divided in the strips using the expressions (1) and (2) because in the earlier investigation [1] is shown that the obtained error is smaller.

The FEM is based on differential equations solving and domain discretization. On the other side, using the EEM, it is necessary to solve only a system of linear equations. Therefore, the EEM calculation time is shorter than the FEM CPU time. Using the FEM is easy to solve problems having a complex geometry and different interfacial boundaries to a degree of accuracy. Only the closed problems can be solved using the FEM. Using the EEM it is possible to solve open electromagnetic problems.

The procedure presented in this article can be applied in the grounding theory, but that will be the task for further investigation. Also, it should be interesting to investigate an influence of equivalent electrodes arrangement on capacitance values.

The obtained results will be good input data for practical application design of this capacitor. After design of such prototype, it will be possible to compare the calculated values with the measured results.

REFERENCES

[1] Aleksić S. R., Marković S. R.: Shallowly-interred ring grounding, XLVIII Conference ETRAN, Čačak, Serbia, 2004, Vol. II, pp. 221-224 (in Serbian).

[2] Aleksić, S. R., Ilić, S. S., Perić, M. T.: Capacitance calculation of “Saturn” capacitor, 7th International Conference on applied electromagnetics ΠΕC 2005, CD Proceedings, Niš, Serbia and Montenegro, 2005, pp. 11-19.

[3] Baumgartner, W., Islas, L., Sigworthierten, F. J.: Two-Microelectrode Voltage Clamp of Xenopus Oocytes: Voltage Errors and Compensation for Local Current Flow, Biophysical Journal, Vol. 77, 1999, pp. 1980-1991.

[4] FEMM 4.0 (“Finite Element Method Magnetics”), David Meeker, 2003.

[5] Perić, M. T., Ilić, S. S.: Capacitance calculation of “Saturn” capacitor, XLIX Conference ETRAN, Budva, Serbia and Montenegro, 2005, Vol. II, pp. 265-267 (in Serbian).

[6] Perić, M. T., Ilić S. S., Aleksić, S. R.: Capacitance calculation of “Saturn” capacitor with finite thickness ring, L Conference ETRAN, Belgrade, Serbia, 2006 (in Serbian).

[7] Perić, M. T., Ilić S. S.: Ring cross-section shape influence on “Saturn” capacitor capacitance, 3rd Int. PhD-Seminar “Computational Electromagnetics and Technical Applications”, Banja Luka, Bosnia and Herzegovina, 2006, pp. 181-186.

[8] Veličković, D. M., Pantić Z. Ž.: A new numerical method for calculating the equivalent radius of uniform antennas, 6th Colloquium on Microwave Communication, Budapest, 1978, pp. III.4/25.1-III.4/25.4.

[9] Veličković, D.: Equivalent Electrodes Method, Scientific Review, Belgrade, 1996, pp. 207-248.

[10] Raičević, N., Aleksić, S.: Electric field regulation at the cable accessories using one new numerical approach, Acta Electrotechnica et Informatica, Vol. 7, No. 1, 2007, pp. 29-36.

[11] Milovanović, A.: An influence of the petrol pump for the atmospheric electric field distribution, Serbian Journal of Electrical Engineering, Vol. 1, No. 3, 2004, pp. 7-14.

[12] Češelkoska, V.: Interaction between LF electric fields and biological bodies, Serbian Journal of Electrical Engineering, Vol. 1, No. 2, 2004, pp. 153-166.

[13] Veličković, D., Zulkić, D., Ilić, S.: Electromagnetic field of coaxial lines with axial slit in a tunnel, in an

enclosed bridge or in a mine pit, Facta Univ. Ser.: Elec. Energ., Vol. 14, No. 2, 2001, pp. 167-185.

[14] Veličković, D. M.: Electrostatic field calculation methods (in Serbian), Stil, Podvis, 1982.

Received January 23, 2009, accepted April 5, 2009

BIOGRAPHIES

Slavoljub R. Aleksić was born in Berčinac, Serbia, in 1951. He enrolled in the Faculty of Electronic Engineering (FEE), University of Niš in 1970. He received Dipl. Ing., M. Sc. and Ph. D. degree at the FEE in 1975, 1979 and 1997, respectively. He employed as a teaching assistant at the Department of Theoretical Electrical Engineering (TEE), after his graduating. He elected for a full professor at the same Department in 2008.
Now, he is a chief of Department of TEE. He is giving one part of lectures for subject Electrical Engineering from 1996. He is also giving the lectures for subject Electromagnetics. He speaks English and Russian.

Mirjana Perić was born in Niš, Serbia, in 1976. She received Dipl. Ing. and M. Sc. degree from the Faculty of Electronic Engineering (FEE), University of Niš, Serbia, in 2000 and 2006, respectively. Since 2001 she has been working as a teaching assistant at the Department of TEE at the FEE in Niš. Her researching areas are: EM field theory, numerical methods in electromagnetics, bioeffects of EM field and program packages application in electromagnetics. She is the author or co-author of a number of published papers.

Saša S. ILIĆ was born in Niš, Serbia, on July 24, 1970. In 1990 he enrolled at the Faculty of Electronic Engineering, University of Niš, Serbia. He chose the electronics and telecommunications major and he received Dipl. Ing. degree in 1995 from the FEE of the University of Niš. From January 1998 up to now, he has engaged to the Department of Theoretical Electrical Engineering, at the FEE of the University of Niš. In 2001 he received M. Sc. degree at the FEE. His researching areas are: lightning protection systems, low-frequency EM fields penetrated into human body and microstrip transmission lines with isotropic, anisotropic and bianisotropic media.